Inorg. Chem. **2003**, *42*, 5143–5152

Structure, Magnetism, and Electrochemistry of the Multinickel Polyoxoanions $[Ni_6As_3W_{24}O_{94}(H_2O)_2]^{17-}$, $[Ni_3Na(H_2O)_2(AsW_9O_{34})_2]^{11-}$, and $[Ni_4Mn_2P_3W_{24}O_{94}(H_2O)_2]^{17-}$

Israel M. Mbomekalle,[†] Bineta Keita,[†] Martine Nierlich,[‡] Ulrich Kortz,*[,§] Patrick Berthet,[||] and Louis Nadjo*[,†]

Electrochimie et Photoélectrochimie, Laboratoire de Chimie Physique, UMR 8000, CNRS, Université Paris-Sud, Bâtiment 420, 91405 Orsay Cedex, France, SCM, CNRS URA 331, CEA Saclay, Bâtiment 125, 91191 Gif-sur-Yvette, France, School of Engineering and Science, International University Bremen, P.O. Box 750 561, 28725 Bremen, Germany, and Laboratoire de Physico-Chimie de l'Etat Solide, UMR 8648, CNRS, Université Paris-Sud, Bâtiment 410, 91405 Orsay Cedex, France

Received April 14, 2003

The three novel, multi-nickel-substituted heteropolytungstates $[Ni_6As_3W_{24}O_{94}(H_2O)_2]^{17-}$ (**1**), $[Ni_3Na(H_2O)_2(AsW_9O_{34})_2]^{11-}$ (**2**), and $[Ni_4Mn_2P_3W_{24}O_{94}(H_2O)_2]^{17-}$ (**3**) have been synthesized and characterized by IR, elemental analysis, electrochemistry, and magnetic studies. Single-crystal X-ray analysis was carried out on $Na_{16.5}Ni_{0.25}[Ni_6As_3W_{24}O_{94}(H_2O)_2]\cdot 54H_2O$, which crystallizes in the triclinic system, space group $P\bar{1}$, with $a = 17.450(4)$ Å, $b = 17.476(4)$ Å, $c = 22.232(4)$ Å, $\alpha = 85.73(3)°$, $\beta = 89.74(3)°$, $\gamma = 84.33(3)°$, and $Z = 2$, $Na_{11}[Ni_3Na(H_2O)_2(AsW_9O_{34})_2]\cdot 30.5H_2O$, which crystallizes in the triclinic system, space group $P\bar{1}$, with $a = 12.228(2)$ Å, $b = 16.743(3)$ Å, $c = 23.342(5)$ Å, $\alpha = 78.50(3)°$, $\beta = 80.69(3)°$, $\gamma = 78.66(3)°$, and $Z = 2$, and $Na_{17}[Ni_4Mn_2P_3W_{24}O_{94}(H_2O)_2]\cdot 50.5H_2O$, which crystallizes in the monoclinic system, space group $P2_1/c$, with $a = 17.540(4)$ Å, $b = 22.303(5)$ Å, $c = 35.067(7)$ Å, $\beta = 95.87(3)$ Å, and $Z = 4$. Polyanion **1** consists of two *B*-α-($Ni_3AsW_9O_{40}$) Keggin moieties linked via a unique AsW_6O_{16} fragment, leading to a banana-shaped structure with C_{2v} symmetry. The mixed-metal tungstophosphate **3** is isostructural with **1**. Polyanion **2** consists of two lacunary *B*-α-$[AsW_9O_{34}]^{9-}$ Keggin moieties linked via three nickel(II) centers and a sodium ion. Electrochemical studies show that **1**–**3** exhibit a unique and reproducible voltammetric pattern and that all three compounds are stable in a large pH range. An investigation of the magnetic properties of **1**–**3** indicates that the exchange interactions within the trimetal clusters are ferromagnetic. However, for **1** and **3** intra- and intermolecular interactions between different trinuclear clusters are also present.

Introduction

Polyoxoanions constitute a rapidly growing class of molecular metal−oxygen clusters with an enormous diversity of structures.[1,2] These molecules also display a unique multitude of properties based on their highly alterable sizes, shapes, charge densities, and reversible redox potentials. As a consequence, possible applications span a wide range of domains including catalysis, electrocatalysis, medicine, materials science, photochemistry, analytical chemistry, and magnetochemistry.[3−6]

* Authors to whom correspondence should be addressed. E-mail: u.kortz@iu-bremen.de (U.K.); louis.nadjo@lcp.u-psud.fr (L.N.). Fax: +49 421 200 3229 (U.K.); +33 1 69 15 43 28 (L.N.).
[†] Laboratoire de Chimie Physique, Université Paris-Sud.
[‡] CEA Saclay.
[§] International University Bremen.
[||] Laboratoire de Physico-Chimie de l'Etat Solide, Université Paris-Sud.

(1) Pope, M. T. *Heteropoly and Isopoly Oxometalates*; Springer-Verlag: Berlin, 1983.
(2) Pope, M. T.; Müller, A. *Angew. Chem., Int. Ed. Engl.* **1991**, *30*, 34−48.
(3) *Polyoxometalates: from Platonic Solids to Anti-Retroviral Activity*; Pope, M. T., Müller, A., Eds.; Kluwer: Dordrecht, The Netherlands, 1994.
(4) *Polyoxometalates*; Hill, C., Ed.; *Chem Rev.* **1998**.
(5) *Polyoxometalate Chemistry: From Topology via Self-Assembly to Applications*; Pope, M. T., Müller, A., Eds.; Kluwer: Dordrecht, The Netherlands, 2001.
(6) *Polyoxometalate Chemistry for Nano-Composite Design*; Yamase, T., Pope, M. T., Eds.; Kluwer: Dordrecht, The Netherlands, 2002.

10.1021/ic0343915 CCC: $25.00
Published on Web 07/31/2003

Incorporation of multiple transition-metal ions in lacunary polyoxoanion fragments can lead to species with various stoichiometries and structural features combined with interesting catalytic and magnetic properties. Frequently novel polyoxoanions with unexpected structures are discovered, which can be traced to the fact that the mechanism of formation of polyoxometalates is not well-understood and commonly described as self-assembly. Therefore, it is necessary to systematically analyze the hitherto mysterious equilibria of polyoxometalates to eventually design straightforward syntheses of novel species.

Within the class of polyoxoanions those species based on trivacant Keggin or Wells−Dawson fragments attract much attention. Several stable and well-characterized sandwich-type polyoxometalates based on such fragments have been known for some time.[7] These species are composed of two *B*-α-$[XW_9O_{34}]^{n-}$ ($n = 7$, X = P^V, As^V; $n = 8$, X = Si^{IV}) or *B*-α-$[X_2W_{15}O_{56}]^{12-}$ (X = P^V, As^V) units and four transition-metal centers. The first example of this structural type, $[Co_4(H_2O)_2(PW_9O_{34})_2]^{10-}$, was reported by Weakley et al., and a few years later Finke et al. reported the first Wells−Dawson derivatives, $[M_4(H_2O)_2(P_2W_{15}O_{56})_2]^{16-}$ (M = Co^{2+}, Cu^{2+}, Zn^{2+}).[7a,c] This series was extended to As(V) derivatives by Evans et al. in the form of the zinc-containing, Keggin-based $[Zn_4(H_2O)_2(AsW_9O_{34})_2]^{10-}$.[7d] Recently Bi et al. described the first arsenic(V) analogues of the Wells−Dawson type, $[M_4(H_2O)_2(As_2W_{15}O_{56})_2]^{16-}$ (M = Mn^{2+}, Co^{2+}, Ni^{2+}, Cu^{2+}, Zn^{2+}, Cd^{2+}).[7p] Also recently Kortz et al. reported the first examples of sandwich-type tungstosilicates, $[M_4(H_2O)_2(SiW_9O_{34})_2]^{12-}$ (M = Mn^{2+}, Cu^{2+}, Zn^{2+}).[7q] These polyanions were synthesized from the dilacunary, metastable precursor [γ-$SiW_{10}O_{36}]^{8-}$. This example is interesting in that it underlines once again the diversity of pathways followed by metastable precursors. Finally, Keita et al. initiated a new series of sandwich-type complexes based on two dissymmetrical lacunary Wells−Dawson ions, $[M_4(H_2O)_2(H_4AsW_{15}O_{56})_2]^{18-}$ (M = Cu^{2+}, Zn^{2+}).[7s]

The first example of a sandwich-type species with fewer than four transition metals has been described recently by Hill et al.[8] The di-iron(III)-substituted polyanion $[Fe_2(NaOH_2)_2(P_2W_{15}O_{56})_2]^{16-}$ is based on two Wells−Dawson fragments, and the two equivalent exterior positions are occupied by sodium ions in the solid state. Hill et al. also showed that this polyanion reacts with Cu^{2+} or Co^{2+} ions in aqueous solution, leading to a trisubstituted mixed-metal sandwich-type polyanion.[9] Very recently the same authors described the tri-iron(III)-substituted polyanion $[Fe_2(FeOH_2)(NaOH_2)(P_2W_{15}O_{56})_2]^{14-}$, which surprisingly is more stable than the tetrairon derivative $[Fe_4(OH_2)_2(P_2W_{15}O_{56})_2]^{12-}$.[10]

Recently we reported the first Keggin-based, trisubstituted, sandwich-type polyoxoanion, $[Ni_3Na(H_2O)_2(PW_9O_{34})_2]^{11-}$.[11] The fourth position in the central plane of this polyanion is occupied by a sodium ion. Interestingly this tri-nickel-substituted polyoxoanion is more stable than its corresponding tetranickel derivative $[Ni_4(H_2O)_2(PW_9O_{34})_2]^{10-}$. This is in agreement with Hill's observations for the tri-iron-substituted Wells−Dawson species.[10]

The nickel-containing tungstophosphates based on the trilacunary [*B*-$PW_9O_{34}]^{9-}$ and [*B*-$P_2W_{15}O_{56}]^{12-}$ fragments can be subdivided into two classes: sandwich type and non-sandwich type. The latter is represented by the monomeric, tetra-nickel-substituted Keggin ion $[H_2PW_9Ni_4O_{34}(OH)_3(H_2O)_6]^{2-}$ and the related mono-tungsten-capped species $[Ni_3(H_2O)_3PW_{10}O_{39}H_2O]^{7-}$.[7o,12] Interestingly all other species belong to the sandwich type and include the dimeric $[Ni_4(H_2O)_2(PW_9O_{34})_2]^{10-}$, $[Ni_4(H_2O)_2(P_2W_{15}O_{56})_2]^{16-}$, and $[Ni_3Na(H_2O)_2(PW_9O_{34})_2]^{11-}$ and the trimeric $[Ni_9(OH)_3(H_2O)_6(HPO_4)_2(PW_9O_{34})_3]^{16-}$.[7k,o,11a]

Recently we have demonstrated that monosubstituted Ni^{2+}- and Cu^{2+}-containing polyoxometalates are effective in the electrocatalytic reduction of nitrates in mildly acidic aqueous media.[13] We have also shown that for this reaction the catalytic effect increases with the number of incorporated nickel centers.

Hence, we believe that multinickel and also mixed-metal polyoxoanion derivatives are very interesting candidates for catalytic applications. Accordingly our synthetic efforts are aimed in the following two directions: (i) synthesis of mixed-metal sandwich-type polyoxoanions with new and/or improved catalytic properties; we decided to use $[Ni_3Na(H_2O)_2(PW_9O_{34})_2]^{11-}$ as a starting material and to attempt replacement of the sodium ion by a redox-active transition metal (e.g., Mn^{2+}); (ii) synthesis of isostructural derivatives of $[Ni_3Na(H_2O)_2(PW_9O_{34})_2]^{11-}$, which could perhaps allow us to fine-tune the catalytic properties. In this context

(7) (a) Weakley, T. J. R.; Evans, H. T. jun.; Showell, J. S.; Tourné, G. F.; Tourné, C. M. *J. Chem. Soc., Chem. Commun.* **1973**, 139. (b) Finke, R. G.; Droege, M.; Hutchinson, J. R.; Gansow, O. *J. Am. Chem. Soc.* **1981**, *103*, 1587. (c) Finke, R. G.; Droege, M. W. *Inorg. Chem.* **1983**, *22*, 1006. (d) Evans, H. T.; Tourné, C. M.; Tourné, G. F.; Weakley, T. J. R. *J. Chem. Soc., Dalton Trans.* **1986**, 2699. (e) Finke, R. G.; Droege, M. W.; Domaille, P. J. *Inorg. Chem.* **1987**, *26*, 3886. (f) Wasfi, S. H.; Rheingold, A. L.; Kokoszka, G. F.; Goldstein, A. S. *Inorg. Chem.* **1987**, *26*, 2934. (g) Weakley, T. J. R.; Finke, R. G. *Inorg. Chem.* **1990**, *29*, 1235. (h) Gómez-García, C. J.; Coronado, E.; Borrás-Almenar, J. J. *Inorg. Chem.* **1992**, *31*, 1667. (i) Casañ-Pastor, N.; Bas-Serra, J.; Coronado, E.; Pourroy, G.; Baker, L. C. W. *J. Am. Chem. Soc.* **1992**, *114*, 10380. (j) Gómez-García, C. J.; Coronado, E.; Gómez-Romero, P.; Casañ-Pastor, N. *Inorg. Chem.* **1993**, *32*, 3378. (k) Gómez-García, C. J.; Borrás-Almenar, J. J.; Coronado, E.; Ouahab, L. *Inorg. Chem.* **1994**, *33*, 4016. (l) Zhang, X.-Y.; Jameson, G. B.; O'Connor, C. J.; Pope, M. T. *Polyhedron* **1996**, *15*, 917. (m) Zhang, X.; Chen, Q.; Duncan, D. C.; Campana, C.; Hill, C. L. *Inorg. Chem.* **1997**, *36*, 4208. (n) Zhang, X.; Chen, Q.; Duncan, D. C.; Lachicotte, R. J.; Hill, C. L. *Inorg. Chem.* **1997**, *36*, 4381. (o) Clemente-Juan, J. M.; Coronado, E.; Galán-Mascarós, J. R.; Gómez-García, C. J. *Inorg. Chem.* **1999**, *38*, 55. (p) Bi, L.-H.; Wang, E.-B.; Peng, J.; Huang, R.-D.; Xu, L.; Hu, C.-W. *Inorg. Chem.* **2000**, *39*, 671. (q) Kortz, U.; Isber, S.; Dickman, M. H.; Ravot, D. *Inorg. Chem.* **2000**, *39*, 2915. (r) Bi, L.-H.; Huang, R.-D.; Peng, J.; Wang, E.-B.; Wang, Y.-H.; Hu, C.-W. *J. Chem. Soc., Dalton Trans.* **2001**, 121. (s) Keita, B.; Mbomekalle I. M.; Nadjo, L.; Contant, R. *Electrochem. Commun.* **2001**, *3*, 267.

(8) (a) Zhang, X.; Anderson, T. M.; Chen, Q.; Hill, C. L. *Inorg. Chem.* **2001**, *40*, 418. (b) Zhang, X.; Hill, C. L. *Chem. Ind.* **1998**, *75*, 519.

(9) Anderson, T. M.; Hardcastle, K. I.; Okun, N.; Hill, C. L. *Inorg. Chem.* **2001**, *40*, 6418.

(10) Anderson, T. M.; Zhang, X.; Hardcastle, K. I.; Hill, C. L. *Inorg. Chem.* **2002**, *41*, 2477.

(11) (a) Kortz, U.; Mbomekalle, I. M.; Keita, B.; Nadjo, L.; Berthet, P. *Inorg. Chem.* **2002**, *41*, 6412. (b) Mbomekalle, I. M.; Keita, B.; Nadjo, L.; Berthet, P. *Inorg. Chem. Commun.* **2003**, *6*, 435.

(12) Kortz, U.; Tézé, A.; Hervé, G. *Inorg. Chem.* **1999**, *38*, 2038.

(13) Keita, B.; Abdeljalil, E.; Nadjo, L.; Contant, R.; Belghiche, R. *Electrochem. Commun.* **2001**, *3*, 56.

substitution of the heteroatom from P(V) to As(V) was an obvious choice.

Here we report some novel polyoxoanions that we have obtained during our research efforts along these directions. In addition to structural details we also present the magnetic and electrochemical properties of all novel species.

Experimental Section

General Methods and Materials. Pure water was used throughout. It was obtained by passing through a RiOs 8 unit followed by a Millipore-Q Academic purification set. All reagents were of high-purity grade and were used as purchased without further purification. Elemental analysis was performed by Kanti Labs Ltd. in Mississauga, Canada. The IR spectra were recorded with KBr pellets on a Perkin-Elmer Spectrum One FT-IR spectrophotometer. Magnetic measurements were carried out on polycrystalline samples using a SQUID magnetometer, Quantum Design MPMS-5. The UV−vis spectra were recorded on a Perkin-Elmer Lambda 19 spectrophotometer on 2.5×10^{-5} M solutions of the relevant polyanion. Matched 1.000 cm optical path quartz cuvettes were used. The compositions of the various media were as follows: for pH 1 to 3, 0.2 M Na_2SO_4 + H_2SO_4; for pH 4 and 5, 0.4 M CH_3COONa + CH_3COOH; for pH 6 and 7, 0.4 M NaH_2PO_4 + NaOH.

Electrochemical Experiments. The same media as for UV−vis spectroscopy were used for electrochemistry, but the polyanion concentration was 2×10^{-4} M. All cyclic voltammograms were recorded at a scan rate of 10 mV·s^{-1}, unless otherwise stated.

The solutions were deaerated thoroughly for at least 30 min with pure argon and kept under a positive pressure of this gas during the experiments. The source, mounting, and polishing of the glassy carbon (GC, Tokai, Japan) electrodes has been described.[14] The glassy carbon samples had a diameter of 3 mm. The electrochemical setup was an EG & G 273 A driven by a PC with the M270 software. Potentials are quoted against a saturated calomel electrode (SCE). The counter electrode was a platinum gauze of large surface area. All experiments were performed at room temperature.

Synthesis of $Na_9[A\text{-}AsW_9O_{34}]\cdot 13H_2O$. A 8.00 g (1.61 mmol) sample of $K_7[H_4AsW_{18}O_{62}]\cdot 18H_2O$ (synthesized according to our recently described procedure)[15] was added to 20 mL of H_2O with stirring at room temperature followed by addition of 8.00 g (57.0 mmol) of $NaClO_4\cdot H_2O$. The solution was vigorously stirred and then cooled in an ice bath for about 2 h. The solid $KClO_4$ that had formed was isolated by filtration, and about 5 g of solid NaCl was added to the yellow filtrate. At this point 25 mL of 1 M Na_2CO_3 solution was added, resulting in slow decoloring of the solution. After about 15 min a white precipitate started to appear, but the solution (pH 8.5) was stirred for another 30 min. Then the precipitate was isolated by filtration and washed consecutively with 1 M NaCl, ethanol, and diethyl ether. The solid was air-dried, resulting in 1.85 g of $Na_9[A\text{-}AsW_9O_{34}]\cdot 13H_2O$ on the basis of infrared spectroscopy and electrochemistry, using the product obtained by the literature method as a reference.[7r] IR for $Na_9[A\text{-}AsW_9O_{34}]\cdot 13H_2O$: 948(s), 848 (vs), 794(s), 703(s), 514(m) cm^{-1}.

Synthesis of $Na_{16.5}Ni_{0.25}[Ni_6As_3W_{24}O_{94}(H_2O)_2]\cdot 54H_2O$ (Na·1) and $Na_{11}[Ni_3Na(H_2O)_2(AsW_9O_{34})_2]\cdot 30.5H_2O$ (Na·2). A 0.630 g (2.65 mmol) sample of $NiCl_2\cdot 6H_2O$ was added with stirring to 50 mL of a 1 M NaCl solution. Then 4.00 g (1.47 mmol) of $Na_9[A\text{-}AsW_9O_{34}]\cdot 13H_2O$ (synthesized as described above) was added in small portions over 5 min. The solution was heated to 60 °C for about 30 min in a water bath and then filtered. The green, clear filtrate was placed in a refrigerator (4 °C). After several months yellow-green crystals were formed (0.30 g, yield 8%) corresponding to the polyanion $[Ni_6As_3W_{24}O_{94}(H_2O)_2]^{17-}$. IR for $Na_{16.5}Ni_{0.25}[Ni_6As_3W_{24}O_{94}(H_2O)_2]\cdot 54H_2O$: 953 (s), 883 (vs), 854 (sh), 754 (vs), 704 (vs), 514 (m) cm^{-1}. Anal. Calcd (Found) for $Na_{16.5}Ni_{0.25}[Ni_6As_3W_{24}O_{94}(H_2O)_2]\cdot 54H_2O$: As, 2.85 (2.87); W, 55.9 (57.3); Ni, 4.65 (4.53); Na, 4.80 (5.16).

After the above product had been filtered off the filtrate was left standing open to the air. A yellow crystalline compound (0.41 g, yield 10%) of the polyanion $[Ni_3Na(H_2O)_2(AsW_9O_{34})_2]^{11-}$ was obtained after several days. IR for $Na_{11}[Ni_3Na(H_2O)_2(AsW_9O_{34})_2]\cdot 30.5H_2O$: 953 (s), 892 (vs), 839 (sh), 726(vs), 511 (m) cm^{-1}. Anal. Calcd (Found) for $Na_{11}[Ni_3Na(H_2O)_2(AsW_9O_{34})_2]\cdot 30.5H_2O$: As, 2.68 (2.75); W, 59.26 (62.5); Ni, 3.15 (3.37); Na, 4.94 (5.53).

Synthesis of $Na_{17}[Ni_4Mn_2P_3W_{24}O_{94}(H_2O)_2]\cdot 50.5H_2O$ (Na·3). A 2.00 g (0.395 mmol) sample of $Na_{11}[Ni_3Na(H_2O)_2(PW_9O_{34})_2]\cdot 14H_2O$ (this compound was first obtained from $K_7[H_4PW_{18}O_{62}]\cdot 18H_2O$, but recently we have described a more direct synthetic procedure)[11] was dissolved in 10 mL of a 1 M NaCl solution with stirring in a water bath (60 °C). Then 80.0 mg (0.404 mmol) of $MnCl_2\cdot 4H_2O$ was added. The solution was heated for about 10 min and then filtered hot. After several days the clear filtrate gave orange crystals (1.50 g, yield 75%) that were recrystallized from 1 M NaCl at room temperature to obtain X-ray-quality crystals. IR for $Na_{17}[Ni_4Mn_2P_3W_{24}O_{94}(H_2O)_2]\cdot 50.5H_2O$: 1040 (s), 1017 (m), 946 (vs), 887 (s), 779 (vs), 727(vs), 589 (w), 514 (m) cm^{-1}. Anal. Calcd (Found) for $Na_{17}[Ni_4Mn_2P_3W_{24}O_{94}(H_2O)_2]\cdot 50.5H_2O$: Ni, 3.05 (3.19); P, 1.21 (1.32); W, 57.37 (58.2); Na, 5.08 (5.4); Mn, 1.43 (1.49).

X-ray Crystallography. A pale yellow, irregular crystal of **Na·1** with dimensions $0.12 \times 0.06 \times 0.06$ mm^3 was mounted onto a glass fiber for indexing and intensity data collection at 123 K. Of the 20908 unique reflections ($R_{int} = 0.215$, $2\theta_{max} = 49.46°$), 7992 were considered observed ($I > 2\sigma(I)$). The final cycle of refinement, including the atomic coordinates, anisotropic thermal parameters (W, As, and Ni atoms), and isotropic thermal parameters (Na and O atoms), converged at $R = 0.089$ and $R_w = 0.155$ ($I > 2\sigma(I)$). In the final difference map the highest peak was 2.890 e Å^{-3} and the deepest hole −2.438 e Å^{-3}.

A colorless, irregular crystal of **Na·2** with dimensions $0.14 \times 0.04 \times 0.02$ mm^3 was mounted onto a glass fiber for indexing and intensity data collection at 123 K. Of the 15966 unique reflections ($R_{int} = 0.111$, $2\theta_{max} = 51.40°$), 9176 were considered observed ($I > 2\sigma(I)$). The final cycle of refinement, including the atomic coordinates, anisotropic thermal parameters (W, As, Ni, and Na1−9 atoms), and isotropic thermal parameters (Na10,11 and O atoms), converged at $R = 0.070$ and $R_w = 0.147$ ($I > 2\sigma(I)$). In the final difference map the highest peak was 3.442 e Å^{-3} and the deepest hole −2.221 e Å^{-3}.

A yellow, irregular crystal of **Na·3** with dimensions $0.15 \times 0.10 \times 0.06$ mm^3 was mounted onto a glass fiber for indexing and intensity data collection at 123 K. Of the 22445 unique reflections ($R_{int} = 0.187$, $2\theta_{max} = 49.44°$), 9908 were considered observed ($I > 2\sigma(I)$). The final cycle of refinement, including the atomic coordinates, anisotropic thermal parameters (W, Ni, P, and Na atoms), and isotropic thermal parameters (O atoms), converged at $R = 0.071$ and $R_w = 0.137$ ($I > 2\sigma(I)$). In the final difference map the highest peak was 2.630 e Å^{-3} and the deepest hole −2.122 e Å^{-3}.

X-ray measurements were performed on a Nonius Kappa CCD single-crystal diffractometer using Mo Kα radiation (λ =

(14) Keita, B.; Girard, F.; Nadjo, L.; Contant, R.; Belghiche, R.; Abbessi, M.; *J. Electroanal. Chem.* **2001**, *508*, 70.
(15) Mbomekalle, I. M. M.; Keita, B.; Nadjo, L.; Contant, R.; Belai, N.; Pope, M. T. *Inorg. Chim. Acta* **2003**, *342*, 219.

Table 1. Crystal Data and Structure Refinement for **Na·1**, **Na·2**, and **Na·3**

	Na·1	Na·2	Na·3
empirical formula	$As_3H_{112}Na_{16.5}Ni_{6.25}O_{150}W_{24}$	$As_2H_{65}Na_{12}Ni_3O_{100.5}W_{18}$	$H_{105}Mn_2Na_{17}Ni_4O_{146.5}P_3W_{24}$
fw	7896.3	5584.8	7690.9
space group (No.)	$P\bar{1}$ (2)	$P\bar{1}$ (2)	$P2_1/c$ (14)
a (Å)	17.450(4)	12.228(2)	17.540(4)
b (Å)	17.476(4)	16.743(3)	22.303(5)
c (Å)	22.232(4)	23.342(5)	35.067(7)
α (deg)	85.73(3)	78.50(3)	
β (deg)	89.74(3)	80.69(3)	95.87(3)
γ (deg)	84.33(3)	78.66(3)	
vol (Å^3)	6728(2)	4554(2)	13646(5)
Z	2	2	4
temp (°C)	−150	−150	−150
wavelength (Å)	0.71073	0.71073	0.71073
d_{calcd} (Mg m^{-3})	3.898	4.089	3.906
abs coeff (mm^{-1})	22.191	24.137	21.087
R^a [$I > 2\sigma(I)$]	0.089	0.070	0.071
$R_w{}^b$ (all data)	0.155	0.147	0.137

^{a} $R = \sum||F_o| - |F_c||/\sum|F_o|$. ^{b} $R_w = [\sum w(F_o^2 - F_c^2)^2/\sum w(F_o^2)^2]^{1/2}$.

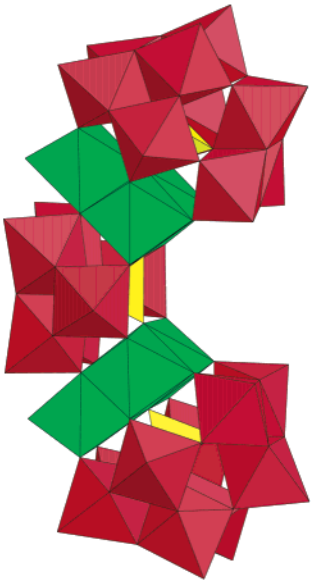

Figure 1. Polyhedral representation of **1**. The AsO_4, WO_6, and NiO_6 polyhedra are shown in yellow, red, and green, respectively.

0.71073 Å). Direct methods were used to solve the structure and to locate the heavy atoms (SHELXS-86). Then the remaining atoms were found from successive difference maps (SHELXL-93). Routine Lorentz and polarization corrections were applied, and an absorption correction was performed using the DELABS program.[16] Crystallographic data are summarized in Table 1.

Results and Discussion

Structures. The novel polyoxoanion $[Ni_6As_3W_{24}O_{94}(H_2O)_2]^{17-}$ (**1**) consists of two *B*-α-($Ni_3AsW_9O_{40}$) Keggin moieties linked via a unique AsW_6O_{16} fragment (see Figures 1 and 2). The arrangement of all three fragments with respect to each other leads to a banana-shaped structure with idealized C_{2v} symmetry. It is also possible to view this polyanion as a double-sandwich structure, which emphasizes the existence of two distinct Ni_3O_{13} triads which are formed

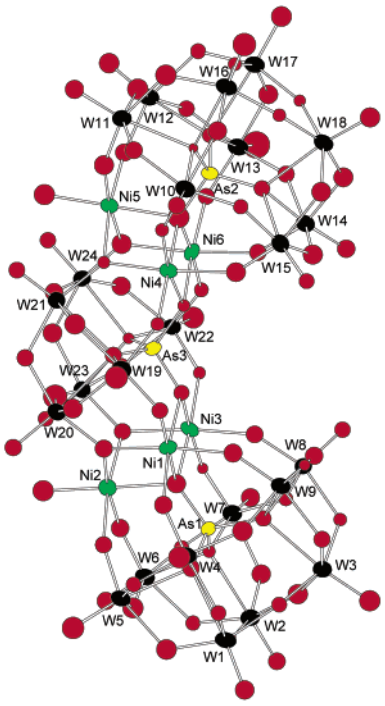

Figure 2. Ball and stick representation of **1** showing 50% probability ellipsoids and the labeling scheme for all atoms except oxygen (for clarity).

from edge-shared NiO_6 octahedra. The trimeric nickel−oxo clusters are separated from each other by the central AsW_6O_{16} tungstoarsenate framework. This polyoxoanion architecture was reported for the first time by Coronado et al. for the cobalt(II)-containing tungstophosphate $[Co_7(H_2O)_2(OH)_2P_2W_{25}O_{94}]^{16-}$.[17] However, in this case, the central, tetrahedral heteroatom position is occupied by an additional cobalt ion and the surrounding metal−oxo fragment contains an extra tungsten atom. The three nickel centers in each triad of **1** are not equivalent, because only one of them has a terminal water molecule. This trinickel fragment resembles that of the recently reported tungstophosphate $[Ni_3Na(H_2O)_2(PW_9O_{34})_2]^{11-}$ (**$Ni_3P_2W_{18}$**) with a sandwich-type structure.[11] However, in this polyanion both capping fragments are composed of a *B*-PW_9O_{34} Keggin moiety, whereas in **1** both capping fragments are different from each other. In fact polyanion **1** can be viewed as an intermediate in the formation of the "regular" trinickel sandwich-type species $[Ni_3Na(H_2O)_2(AsW_9O_{34})_2]^{11-}$ (**2**); see Figures 3 and 4. Interestingly we were also able to obtain this polyanion from the filtrate of the same reaction mixture after **1** had been isolated. Polyanion **2** can be viewed as the arsenic-containing analogue of **$Ni_3P_2W_{18}$**, and like the latter it also contains a sodium ion in addition to the three nickel ions in the central plane of the structure. Although the arsenic(V) heteroatom is larger than phosphorus(V), we were able to obtain isomorphous crystal structures for both compounds.[18] This means that the difference in bond lengths between As−O (d = 1.65−1.74(2) Å) and P−O (d = 1.51−1.56(2) Å) has

(16) Spek, A. L. *PLATON*; University of Utrecht, Utrecht, The Netherlands, 1998.

(17) Borras-Almenar, J. J.; Clemente-Juan, J. M.; Clemente-Leon, M.; Coronado, E.; Galan-Mascaros, J. R.; Gomez-Garcia, C. J. In *Polyoxometalate Chemistry: From Topology via Self-Assembly to Applications*; Pope, M. T., Müller, A., Eds.; Kluwer: Dordrecht, The Netherlands, 2001; p 231.

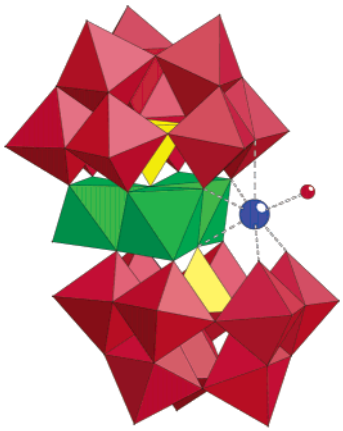

Figure 3. Combined polyhedral/ball-and-stick representation of **2**. The AsO_4, WO_6, and NiO_6 polyhedra are shown in yellow, red, and green, respectively. The sodium atom is shown as a blue ball and its terminal water molecule as a red ball.

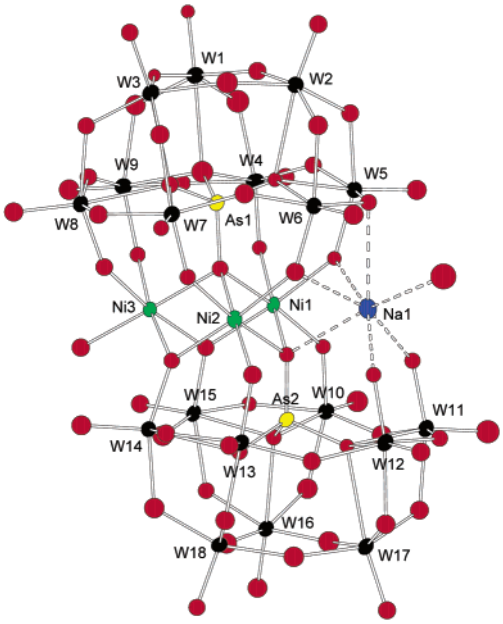

Figure 4. Ball-and-stick representation of **2** showing 50% probability ellipsoids and the labeling scheme for all atoms except oxygen (for clarity).

no significant effect on the surrounding metal−oxo framework. Polyanion **2** represents the first example of a trisubstituted tungstoarsenate with a sandwich-type structure.

The two Ni_3O_{13} clusters in polyanion **1** are crystallographically independent, because the entire molecule is present in the asymmetric unit. All nickel centers are octahedrally coordinated, the nickel−oxygen distances are as expected (1.95−2.17(4) Å), and the bond lengths and angles of the tungsten−oxo frameworks are within the usual ranges. Bond-valence sum calculations confirm that the terminal water molecules of Ni2 and Ni5 are the only protonated oxygens of **1**.[19] This leads to a charge of 17− for **1**, which has to be balanced by the appropriate number of countercations in the lattice. We were able to account for only 9.5 sodium ions by X-ray diffraction (XRD), which was not unexpected because of disorder. However, by XRD we also identified unequivocally the presence of a minute amount of nickel(II) as counterion, accounting for about 25% of a nickel ion for each polyanion. This observation was confirmed and the total assembly of counterions in the lattice of **Na·1** ($16.5Na^+$ and $0.25Ni^{2+}$) was established by elemental analysis.

As described above polyanions **1** and **2** resulted from the same synthetic procedure. Most likely both species coexist in solution as a result of interaction of Ni^{2+} ions with the trivacant Keggin isomer of the *A* type, $[A\text{-}AsW_9O_{34}]^{9-}$. However, due to their different solubility characteristics we could obtain pure samples of **1** and **2** by fractional crystallization. Both polyanions **1** and **2** were isolated in very similar (low) yields, which does not allow one of them to be considered as a minor byproduct of the other. It must be remembered that during the original synthesis of $\mathbf{Ni_3P_2W_{18}}$ we also obtained a byproduct, which was however the trimeric $[Ni_9(OH)_3(H_2O)_6(HPO_4)_2(PW_9O_{34})_3]^{16-}$ rather than the hypothetical species $[Ni_6P_3W_{24}O_{94}(H_2O)_2]^{17-}$ (which is still unknown).

The original motivation for the work that has led to **1** and **2** was based on the idea to synthesize the arsenic-containing analogue of $\mathbf{Ni_3P_2W_{18}}$. Therefore, we decided to perform the synthesis in complete analogy to that of the phosphorus-containing polyanion. We synthesized the $[A\text{-}AsW_9O_{34}]^{9-}$ precursor from $[H_4AsW_{18}O_{62}]^{7-}$ (following our method described recently) rather than using the procedure of Wang and co-workers.[7r] Then we reacted the trilacunary $[A\text{-}AsW_9O_{34}]^{9-}$ with nickel(II) ions in aqueous acidic medium. Both products from this reaction (**1** and **2**) contain $[B\text{-}AsW_9O_{34}]^{9-}$ fragments, which means that during the course of the reaction the following isomerization must have taken place: $[A\text{-}AsW_9O_{34}]^{9-} \rightarrow [B\text{-}AsW_9O_{34}]^{9-}$. Therefore, we have shown for the first time that the *A*-isomer of $[AsW_9O_{34}]^{9-}$ isomerizes to the *B*-isomer in aqueous acidic medium at 60 °C, which is in complete agreement with the observations of Knoth et al. for the phosphorus analogue.[20] Recently Wang et al. have also shown that $[A\text{-}AsW_9O_{34}]^{9-}$ can be transformed to $[B\text{-}AsW_9O_{34}]^{9-}$ in the solid state, under conditions very similar to those of the P-containing analogue.[7r,21]

The mixed-metal polyanion $[Ni_4Mn_2P_3W_{24}O_{94}(H_2O)_2]^{17-}$ (**3**) is isostructural with **1** (see Figure 1), although both resulted from different synthetic procedures. The former was synthesized by interaction of $\mathbf{Ni_3P_2W_{18}}$ with 1 equiv of Mn^{II} ions with the original aim to substitute the sodium ion by a first-row transition metal different from nickel. We have discovered that for manganese(II) ions this substitution reaction is not straightforward, because it is accompanied by an unexpected rearrangement of the polyoxoanion framework, resulting in **3**. It is known that the incorporated sodium

(18) Our first structural report of the tungstophosphate $[Ni_3Na(H_2O)_2(PW_9O_{34})_2]^{11-}$ was based on $Na_{11}[Ni_3Na(H_2O)_2(PW_9O_{34})_2]\cdot 21.25H_2O$.[11a] Recently we crystallized the slightly different hydrate $Na_{11}[Ni_3Na(H_2O)_2(PW_9O_{34})_2]\cdot 29.5H_2O$, which is isomorphous with **Na·2** presented here.

(19) Brown, I. D.; Altermatt, D. *Acta Crystallogr.* **1985**, *B41*, 244.

(20) Knoth, W. H.; Domaille, P. J.; Harlow, R. L. *Inorg. Chem.* **1986**, *25*, 1577.

(21) Domaille, P. J. *Inorganic Syntheses*; John Wiley & Sons: New York, 1990; Vol. 27, p 100.

ion plays an important stabilizing role for the tri-nickel-substituted species $\mathbf{Ni_3P_2W_{18}}$. Therefore, it could be possible that this sodium- and tri-nickel-substituted species is not reactive enough under our rather mild reaction conditions. Nevertheless, we have experimental evidence that some mixed-metal derivatives of $\mathbf{Ni_3P_2W_{18}}$ can be formed easily. However, the substitution appears to be more facile with some transition-metal ions than with others. A detailed study of this phenomenon is currently in progress, and the results will be discussed elsewhere.

Polyanion **3** can be obtained within days in very good yield, which is in marked contrast to **1** and **2**. Therefore, it appears that the rearrangement of $\mathbf{Ni_3P_2W_{18}}$ to **3** is rather "clean" and probably catalyzed by manganese(II) ions. Most likely we isolated **3** rather than $[Ni_3Mn(H_2O)_2(PW_9O_{34})_2]^{10-}$ because the former is more stable than the latter under our reaction conditions. Nevertheless, it is very likely that $[Ni_3Mn(H_2O)_2(PW_9O_{34})_2]^{10-}$ is present as an intermediate in the formation mechanism of **3** starting from $\mathbf{Ni_3P_2W_{18}}$.

The presence of four nickel(II) and two manganese(II) ions in **3** could not be identified by X-ray diffraction, but it was clearly established by a combination of elemental analysis, electrochemistry, and magnetic measurements. The exact distribution of the six transition-metal ions among the two M_3O_{13} triads of **3** is a tricky issue, but we have experimental evidence that each transition-metal cap consists of one Mn^{2+} ion and two Ni^{2+} ions. However, we cannot assign the manganese ions to a specific position within each M_3O_{13} triad in **3**. It must be realized that within each triad there are two distinct positions (ratio 2:1) that each manganese ion could occupy. The idealized C_{2v} symmetry of **1** would only be preserved by **3** if both manganese ions in **3** occupied the two positions assigned as Ni2 and Ni5 in the all-nickel derivative **1** (see Figure 2). Whether indeed different positional isomers of **3** are present is very difficult to identify experimentally.

Magnetism. For **1**−**3** the temperature dependence of the magnetization was studied in a 0.1 T field: the $X_{mol}T$ values deduced from this study are plotted as a function of T in Figure 5. For each compound under study, the $X_{mol}T$ product shows a maximum which is found between 4 and 12 K. These maxima are characteristic of ferromagnetic exchange interactions between the metal atoms within each trinuclear fragment.[7k,o] Moreover, for **1** and **3** some intramolecular magnetic coupling may exist between the two trinuclear clusters. At lower temperature, the $X_{mol}T$ values decrease with decreasing temperature, which suggests antiferromagnetic interactions between neighboring polyoxoanions. At high temperature, the $X_{mol}T$ values have an asymptotic behavior characteristic of three (**2**) or six (**1**, **3**) independent paramagnetic ions in each compound.

For a quantitative analysis of the magnetic interactions, the experimental susceptibility of **2** and $\mathbf{Ni_3P_2W_{18}}$ may be written as

$$X_{mol} = [T/(T - T_{CW})X_{cluster}] + X_0$$

where T_{CW} is the negative Curie−Weiss temperature accounting for the mean field corrections associated with antiferromagnetic intercluster interactions, X_0 represents temperature-independent contributions mainly due to the diamagnetism of the tungsten−oxo framework, and $X_{cluster}$ is the intrinsic susceptibility of the trinuclear cluster. The latter is given by the following equation:

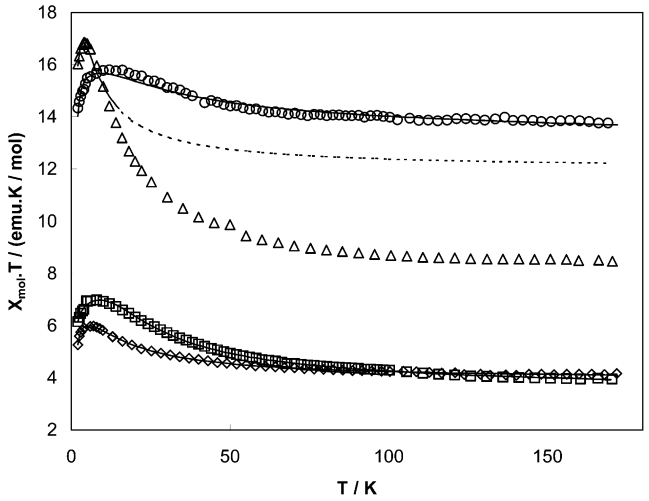

Figure 5. $X_{mol}T$ as a function of T. The data corresponding to the different compounds are represented by squares ($\mathbf{Ni_3P_2W_{18}}$), tilted squares (**2**), triangles (**1**), and circles (**3**). The continuous lines represent the least-squares fits to the data using parameters reported in Table 2. The dashed line is the extrapolation of the low-temperature fit relative to **1**.

$$X_{cluster} = g^2N\beta^2\langle S_T(S_T + 1)\rangle/3kT$$

in which the mean value $\langle S_T(S_T + 1)\rangle$ depends on the temperature which determines the population of the energy levels resulting from the individual spin coupling. Assuming that at least two of the magnetic interactions between the three Ni^{II} ions are identical, the magnetic energy of the cluster can be described by the following Heisenberg-type Hamiltonian:

$$\hat{H} = -2J_1(\hat{S}_1\cdot\hat{S}_2 + \hat{S}_1\cdot\hat{S}_3) - 2J_2\hat{S}_2\cdot\hat{S}_3$$

The eigenvalues of this Hamiltonian operator are obtained by the vector-coupling method of Kambe:[22]

$$E(S_T,S_{23}) = -J_1[S_T(S_T + 1) - S_{23}(S_{23} + 1) - S_1(S_1 + 1)] - J_2[S_{23}(S_{23} + 1) - S_2(S_2 + 1) - S_3(S_3 + 1)]$$

where S_{23} and S_T are related to the spin operators $\hat{S}_{23} = \hat{S}_2 + \hat{S}_3$ and $\hat{S}_T = \hat{S}_{23} + \hat{S}_1$.

For a system of three spins of 1, there are seven (S_T, S_{23}) combinations of energy E_i, which led to

$$\langle S_T(S_T+1)\rangle = \sum a_i \exp(-E_i/kT)/\sum b_i \exp(-E_i/kT)$$

with $b_i = 2S_T(E_i) + 1$ and $a_i = b_iS_T(E_i)(S_T(E_i) + 1)$.

By fitting the calculated to the experimental $X_{mol}T$ values, it is possible to determine the magnetic parameters describing the cluster (Table 2). For **2** and $\mathbf{Ni_3P_2W_{18}}$ these parameters lead to an $S = 3$ ground state well-separated from the first

(22) Kambe, K. *J. Phys. Soc. Jpn.* **1950**, *5*, 48.

Table 2. Magnetic Parameters and First Energy Levels for **1**−**3** and **$Ni_3P_2W_{18}$**

	$Ni_3P_2W_{18}$	**2**	**1**[a]	**3**
g_L	2.22	2.28	2.00	2.07
J_1 (cm^{-1})	4.5	4.2	0.33	0.19
J_2 (cm^{-1})	4.5	−1.0	−	7.2
T_{CW} (K)	−0.40	−0.80	−0.59	−1.36
X_0 (emu·mol^{-1})	-7.5×10^{-4}	-8×10^{-6}	0	-1.7×10^{-3}
E_0 (cm^{-1}) (S_T, S_{23})	−27.1 (3, 2)	−15.0 (3, 2)	−5.9 (6)	−16.3 (9/2, 2)
E_1 (cm^{-1}) (S_T, S_{23})	0 (2, 2; 2, 1)	−10.4 (2, 1)	−2.0 (5)	−14.6 (7/2, 2)

[a] For **1**, the results are related to the magnetic coupling of two $S = 3$ units and X_0 was fixed to 0 since its exact value has a negligible effect on low-temperature data.

excited state. The Curie−Weiss temperatures are close to that (−0.65 K) reported by Coronado and co-workers for a closely related Ni^{II} tetranuclear cluster.[7k] However, it is worth noting that in more recent work these investigators have shown that the behavior of $X_{mol}T$ at very low temperature may be related to an anisotropic coupling of the Ni^{II} ions inside the cluster rather than to a mean field correction.[7o] With this alternative explanation, T_{CW} appears as a parameter describing the zero-field splitting of the local Ni^{II} spins. As can be observed in Figure 5, the $X_{mol}T$ maximum value is higher for **$Ni_3P_2W_{18}$** than for **2**. This difference is clearly related to the J_i interaction parameters obtained from the fitting procedure. For **$Ni_3P_2W_{18}$** the experimental data are satisfactorily reproduced with a single parameter, whereas two different parameters, J_1 and J_2, were necessary for **2**. Moreover, J_2 is found to be negative, and such an antiferromagnetic coupling may seem surprising, but it has already been observed by Gladfelter and collaborators in a tetranuclear cubane structure.[23] According to these investigators, the magnetic interaction is highly sensitive to the value of the Ni−O−Ni bridging angle: the interactions are ferromagnetic for angles close to 90°, whereas they are antiferromagnetic for slightly larger angles. A comparison of the structural parameters obtained in the present study shows that such an explanation is satisfying: the Ni−O−Ni angles are larger in **2** than in **$Ni_3P_2W_{18}$**. For example, the smallest Ni−O−Ni angle in **2** has a value of 95.6° versus 92.1° in **$Ni_3P_2W_{18}$**, and the mean values of all the bridging angles are, respectively, 98.4° and 96.6°. However, one cannot exclude partial decomposition of **Na·2** upon drying, which could have significant consequences on its low-temperature magnetic properties.

The study of the field dependence of the magnetization of both compounds recorded at 2 K (Figure 6) confirms the difference existing between them. The increase of the magnetization with the applied field is faster for **$Ni_3P_2W_{18}$** than for **2**, whereas the saturation magnetization appears higher for the latter. For both compounds, attempts were made to reproduce the data with a Brillouin function taking into account mean field corrections similar to those represented by T_{CW} in the analyses of $X_{mol}T$. For this purpose, the experimental magnetizations were first parametrized by the following equation: $m = \alpha \tan^{-1}(\mathbf{H}/\beta)$, and the applied field **H** was replaced by $(H - wm)$, where w is the mean field coefficient. For a given spin state, modelization with a Brillouin function depends on the value of the Lande g factor. A minimum value of this factor may be deduced from the magnetization at high field since at saturation $M_S = gS$. With this constraint, the value of the w mean field coefficient was determined from the low-field linear part of the magnetization. For **$Ni_3P_2W_{18}$** this attempt appears unsuccessful since the minimum value of the g factor required to account for the low-field magnetization is 2.08, which gives $w = 0$. However, the highest value of the g factor (2.22) deduced from the analysis of $X_{mol}T$ gives $w = 213$ Oe/emu. In both cases, the calculated magnetization becomes significantly higher than the experimental one for fields higher than 5000 Oe. For **2** the minimum value of the g factor deduced from the high-field magnetization (2.16) leads to $w = 444$ Oe/emu, whereas the value obtained from the $X_{mol}T$ products (2.28) leads to $w = 607$ Oe/emu. For **$Ni_3P_2W_{18}$** the agreement is rather poor between the calculated values and the experimental data. These discrepancies indicate that a mean field approach represented by a single parameter such as w or T_{CW} is only convenient at low field. At higher field a different approach should be followed; it could require a more complex description of the antiferromagnetic interactions or of a possible anisotropic coupling of the Ni^{II} ions in the cluster.

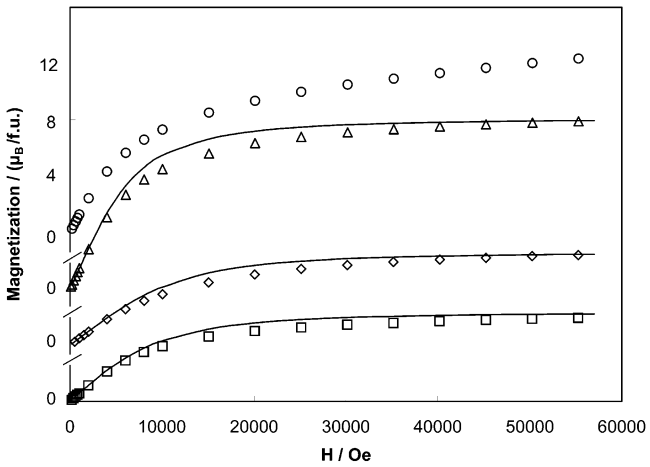

Figure 6. Magnetizations as a function of the applied field, recorded at 2 K. The data corresponding to the different compounds are represented by squares (**$Ni_3P_2W_{18}$**), tilted squares (**2**), triangles (**1**), and circles (**3**). The continuous lines represent Brillouin functions for the $S = 3$ (**$Ni_3P_2W_{18}$**, **2**) or $S = 6$ (**1**) state and the lowest mean field corrections reported in the text.

Interpretation of the temperature dependence of the $X_{mol}T$ values for **1** and **3** has to take into account possible intramolecular interactions between the two trimetal clusters. For **1** the maximum value (16.9 emu·K·mol^{-1}) of the product $X_{mol}T$ suggests a ferromagnetic interaction, since for two independent $S = 3$ clusters it would correspond to a g factor of 2.38, noticeably higher than those determined for the single-cluster compounds. Moreover, such a value for the g factor would give a saturation magnetization of 14.2 μ_B per formula unit, clearly higher than the high-field data (Figure 6), which are close to 12 μ_B per formula unit. To check this hypothesis, one can try to reproduce the low-temperature data

(23) Gladfelter, W. L.; Lynch, M. W.; Schaefer, W. P.; Hendrickson, D. N.; Gray, H. B. *Inorg. Chem.* **1981**, *20*, 2390.

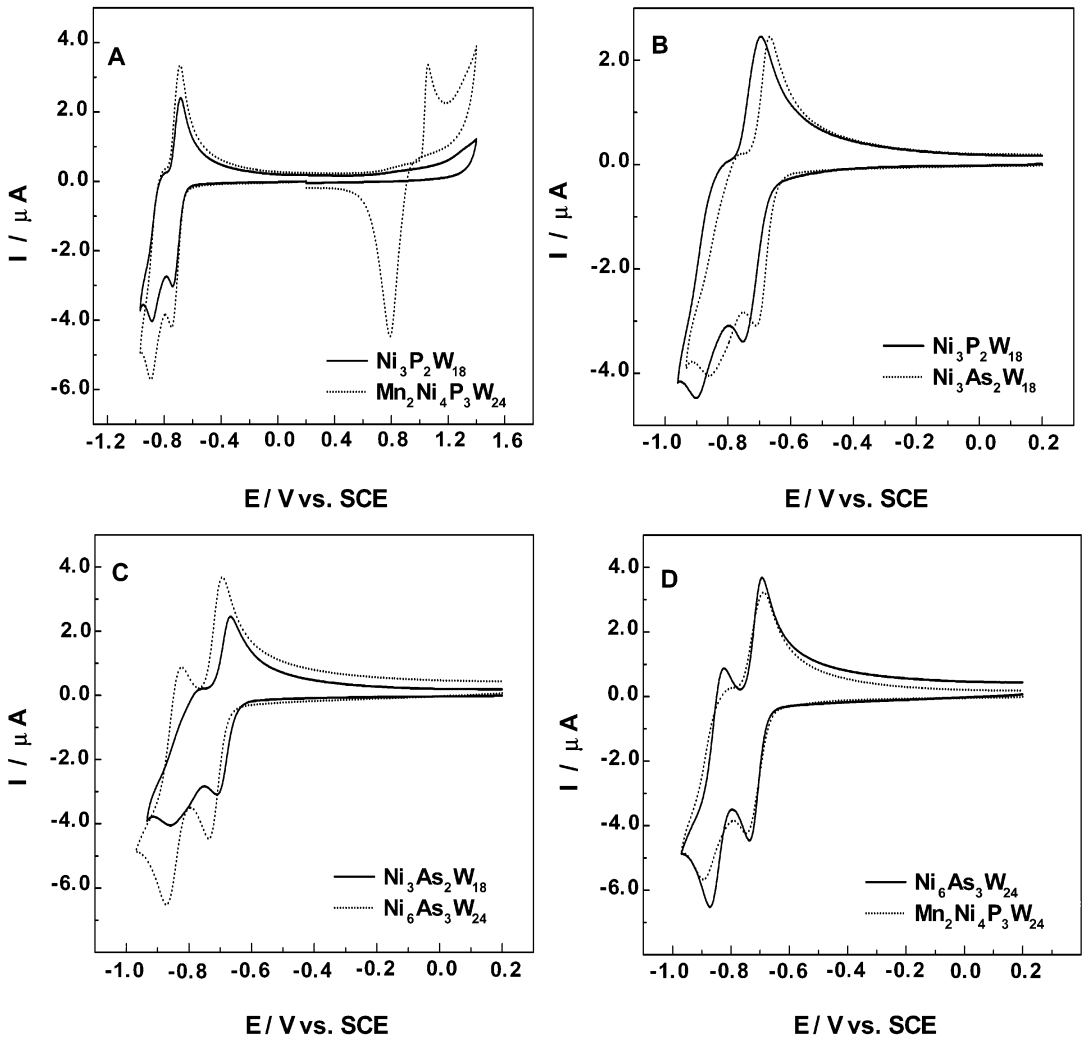

Figure 7. (A) Comparison of the cyclic voltammograms of 2×10^{-4} M **$Ni_3P_2W_{18}$** and **3**, at pH 3 (0.2 M $Na_2SO_4 + H_2SO_4$) (scan rate, 10 mV·s^{-1}; working electrode, polished glassy carbon; reference electrode, SCE). For further details, see the text. (B) Comparison of the cyclic voltammograms of 2×10^{-4} M **$Ni_3P_2W_{18}$** and **2**, at pH 3 (0.2 M $Na_2SO_4 + H_2SO_4$) (scan rate, 10 mV·s^{-1}; working electrode, polished glassy carbon; reference electrode, SCE). For further details, see the text. (C) Comparison of the cyclic voltammograms of 2×10^{-4} M **2** and **1**, at pH 3 (0.2 M $Na_2SO_4 + H_2SO_4$) (scan rate, 10 mV·s^{-1}; working electrode, polished glassy carbon; reference electrode, SCE). For further details, see the text. (D) Comparison of the cyclic voltammograms of 2×10^{-4} M **1** and **3**, at pH 3 (0.2 M $Na_2SO_4 + H_2SO_4$) (scan rate, 10 mV·s^{-1}; working electrode, polished glassy carbon; reference electrode, SCE). For further details, see the text.

as resulting from the coupling of two $S = 3$ spins, using the formalism described above. A satisfying agreement with experiment is obtained with the parameters reported in Table 2 for temperatures lower than 15 K. This approach is not convenient for higher temperature since thermal disorder leads to a decrease of the mean spin of each cluster. The low- and high-field dependence of the magnetization at 2 K can be described by a Brillouin function corresponding to an $S = 6$ state with mean field correction ($w = 164$ Oe/μ_B for $g = 2$) but as for the previous polyanions this description is not satisfying at intermediate field. For **3** the maximum value (15.8 emu·K·mol^{-1}) of the $X_{mol}T$ product is rather low, since for two independent Ni_2Mn clusters a value of 24.75 emu·K·mol^{-1} would be expected for a high-spin configuration with a g factor equal to 2 (and an even higher value in the case of ferromagnetic coupling between the trinuclear clusters). As a strong coupling between the two internal clusters may be discarded, it is possible to analyze the experimental data in the same way as that followed for the single-cluster compounds. Inside a cluster, the magnetic interactions between the Mn^{II} ion and both Ni^{II} ions are described by the exchange parameter J_1 and coupling between the two Ni^{II} ions is described by J_2. Examination of the refined parameters reported in Table 2 clearly shows that interaction of the Mn^{II} and Ni^{II} ions is clearly weaker than that of the two Ni^{II} ions. Moreover, the antiferromagnetic intermolecular interaction represented by T_{CW} appears stronger than those found for the single-cluster complexes. This strength may explain that saturation is difficult to reach in the study of the field dependence of the magnetization (Figure 6). For this sample it is impossible to reproduce the data with a Brillouin function and a mean field correction. This suggests that at low field T_{CW} simultaneously represents intramolecular interactions between the two internal trimetal clusters of each polyanion and intermolecular interactions between different polyanions.

Electrochemistry. $[Ni_4Mn_2P_3W_{24}O_{94}(H_2O)_2]^{17-}$ (3). Figure 7A compares, in a pH 3 medium, the cyclic voltammo-

grams of **3** and of the original precursor used for its synthesis, $\mathbf{Ni_3P_2W_{18}}$. The cyclic voltammogram of the latter species was described in a recent paper and is added here for the sake of direct comparison of the two complexes.[11a] In the negative potential domain, only the first two redox couples located just before proton reduction are represented. The cyclic voltammograms of the two complexes are very similar in shape, with the pattern for **3** located slightly more negatively in potential. This observation might be traced to the difference in the overall negative charges of the complexes. As a matter of fact, with the assumption that all other factors act practically in the same way, it is expected that **3** with 17 negative charges should be more difficult to reduce than $\mathbf{Ni_3P_2W_{18}}$ with only 12 negative charges.[1] It must be noted, however, that the magnitude of this difference might be modulated by acidobasic properties of the reduced forms of the complexes. As observed previously for $\mathbf{Ni_3P_2W_{18}}$, these two waves are attributed to redox processes of W^{VI} centers. In the positive potential domain, only **3** shows a wave with a peak located at +1.058 V, featuring the oxidation of Mn^{II} centers.

$[Ni_6As_3W_{24}O_{94}(H_2O)_2]^{17-}$ (1) and $[Ni_3Na(H_2O)_2(AsW_9O_{34})_2]^{11-}$ (2). The cyclic voltammogram of **2** is also constituted by two reversible waves that are located in a more positive potential domain than that of its P analogue $\mathbf{Ni_3P_2W_{18}}$ as shown in Figure 7B. This observation is in agreement with results on other heteropolyanions for which the presence of As instead of P as the central heteroatom facilitates the reduction process.[24] In analogy to the case of $\mathbf{Ni_3P_2W_{18}}$, the second wave is followed by the reduction of protons. Furthermore, controlled potential coulometric determination at −0.730 V in a pH 3 medium confirms that four electrons are consumed per molecule in the first wave, as already observed previously for the P analogue.[11a] In short, the electrochemical and IR characterizations as well as elemental analysis converge to confirm that **2** and $\mathbf{Ni_3P_2W_{18}}$ have the same structure.

On the basis of cyclic voltammetry, it is possible to clearly distinguish **1** and **2** as shown in Figure 7C. In agreement with the difference in charges of the two polyanions, the more heavily negative one, **1**, is slightly more difficult to reduce than **2**. As the two molecules are not expected to have the same diffusion coefficient, the simple comparison of the peak current intensities of the respective cyclic voltammograms of **1** and **2** cannot be used for an accurate determination of the number of electrons on the latter species. Nevertheless, it can be easily concluded that this number of electrons is larger for **1**. Figure 7D compares the cyclic voltammograms of **1** and **3**, and as expected the compound with P as the heteroatom is more difficult to reduce than its As analogue.[24] These two polyanions are likely to have fairly similar diffusion coefficients; therefore, their cyclic voltammograms can be compared straightforwardly and correspond to the same number of electrons, albeit for the potential locations. Controlled potential coulometry performed at pH 3 on the first W wave of these two compounds indicates that these waves correspond to six-electron processes for each polyanion.

Table 3. Cyclic Voltammetry Reduction Peak Potentials as a Function of pH for **1**−**3** and $\mathbf{Ni_3P_2W_{18}}$[a]

compd	pH	$-E_{pc}$(first W wave) (V)	$-E_{pc}$(second W wave) (V)
2	3	0.710	0.854
	5	0.856	0.994
$\mathbf{Ni_3P_2W_{18}}$	3	0.738	0.882
	5	0.866	1.028
1	3	0.736	0.870
	5	0.910	1.026
3[b]	3	0.746	0.892
	5	0.912	1.040

[a] Working electrode, glassy carbon; scan rate, 10 $mV \cdot s^{-1}$; reference electrode, SCE. For further details, see the text. [b] Mn oxidation processes were observed at +1.058 V (pH 3) and +0.880 V (pH 5).

pH Effects. To our knowledge all Ni-rich sandwich-type complexes in the literature except for $\mathbf{Ni_3P_2W_{18}}$ show narrow stability pH domains.[7o,20] This led us to study the stability of **1**−**3** between pH 1 and 7. For this purpose, the UV−vis spectrum of each polyanion was measured and compared with that obtained after 24 h of standing. At pH 2 the maximum absorption was found at 255 nm for **1**, and was broad and located between 240 and 250 nm for **2** and **3**. The exact energies and shapes vary slightly with the pH of the medium. This period of time is substantially longer than necessary for electrochemical characterizations and also allows for eventual electrocatalytic applications to be envisioned. Typically, all three compounds were found to be stable from pH 2 to pH 6. Furthermore, $\mathbf{Ni_3P_2W_{18}}$ was stable at least down to pH 1. For **1**, the stability domain spans from pH 1 to pH 7 and might even be larger.

In analogy to $\mathbf{Ni_3P_2W_{18}}$ polyanions **1**−**3** are sufficiently stable between pH 2 and pH 6 to be good candidates for applications in electrocatalysis. Furthermore, variations of the characteristics of their cyclic voltammograms as a function of pH comply with what is known from current literature for various types of heteropolyanions. The reduction peak potential values in Table 3 illustrate such behavior for the cyclic voltammograms of all compounds recorded at pH 3 and 5. As expected, the reduction waves of the W^{VI} centers are driven in the negative potential direction when the pH is changed from 3 to 5; concomitantly, the Mn^{II} oxidations also become less positive in potential. Again, those complexes containing As heteroatoms remain easier to reduce than their P analogues. It is of interest to compare the electrochemical behavior of **3** with that of the tetramanganese(II)-substituted sandwich-type tungstophosphate $[Mn_4(H_2O)_2(PW_9O_{34})_2]^{10-}$. A few years ago Pope et al. studied the oxidation properties of this polyanion in detail and discovered that oxidation occurs first at the aquated Mn centers.[7l] Our observation that the oxidation of **3** is pH dependent supports the preliminary conclusion that the two manganese centers also contain a water ligand. This would suggest that the Mn^{II} ions occupy the two unique, external positions in **3** (see Figures 1 and 2).

A final point deserves emphasis: whatever the pH, it was observed that the anodic to cathodic peak potential differ-

(24) Keita, B.; Mbomekalle, I. M.; Nadjo, L.; Contant, R. *Eur. J. Inorg. Chem.* **2002**, 473.

ences for these multielectron waves were between 42 and 76 mV in the present experiments. In other words, the relevant systems behave roughly as one-electron systems, except for the current intensity. These complexes might be considered as assemblies of identical moieties linked together by a central metal layer for sandwich-type species or a more extended linkage for others. These observations suggest that these centers are largely independent and are reduced simultaneously, a feature reminiscent of the reduction of polymers or dendrimers.[25,26] Work in progress will elaborate on such systems in more detail.

Conclusion

We have synthesized and structurally characterized two nickel-substituted tungstoarsenates and one mixed-metal (Ni, Mn) tungstophosphate. The sandwich-type polyanion $[Ni_3Na(H_2O)_2(AsW_9O_{34})_2]^{11-}$ resulted from a successful attempt to prepare the As analogue of $[Ni_3Na(H_2O)_2(PW_9O_{34})_2]^{11-}$. This result further supports the observation that for many tungstophosphates(V) the analogous tungstoarsenates(V) are known, a similarity which is not at all true for the P and As heteroatoms being in the lower oxidation state III. Unexpectedly we also obtained the banana-shaped species $[Ni_6As_3W_{24}O_{94}(H_2O)_2]^{17-}$ during the same synthesis, but both compounds could be isolated in a pure form by fractional crystallization. Bulk samples of the tungstoarsenates were characterized by a multitude of experimental techniques including elemental analysis, electrochemistry, and magnetic studies. Most likely $[Ni_6As_3W_{24}O_{94}(H_2O)_2]^{17-}$ is an intermediate during the formation of $[Ni_3Na(H_2O)_2(AsW_9O_{34})_2]^{11-}$. Unfortunately both compounds could only be isolated in low yields, which leaves the question of what exactly the species remaining in solution are. Therefore, we continue to work on this system to optimize the synthetic conditions and hopefully to get a better understanding of the mechanism of formation of both tungstoarsenates.

The mixed nickel−manganese tungstophosphate $[Ni_4Mn_2P_3W_{24}O_{94}(H_2O)_2]^{17-}$ is isostructural with $[Ni_6As_3W_{24}O_{94}(H_2O)_2]^{17-}$ but resulted from an attempt to prepare the sandwich-type, mixed-metal species $[Ni_3Mn(H_2O)_2(PW_9O_{34})_2]^{10-}$ by reaction of the well-known $[Ni_3Na(H_2O)_2(PW_9O_{34})_2]^{11-}$ with manganese(II) ions. The very good yield with which $[Ni_4Mn_2P_3W_{24}O_{94}(H_2O)_2]^{17-}$ was isolated seems to indicate that the two manganese ions should occupy two unique positions in this polyanion structure. Although we have characterized this compound by several analytical techniques, we cannot identify unequivocally which of the six possible 3d metal positions of the polyanion structure are occupied by Mn^{2+} ions and also cannot rule out Mn/Ni disorder. However, on the basis of electrochemistry, we strongly believe that the two Mn^{2+} ions occupy the two unique and equivalent positions described as Ni2 and Ni5 in Figure 2.

The similarity of polyanion structures synthesized under a priori very different starting conditions and containing different heteroatoms in the precursor species underscores the complexity of the subtle interactions and equilibria in aqueous solution that may result in the formation of stable heteropolyanions. Our discovery of novel and unexpected polyanion architectures once again reemphasizes the virtually unlimited structural variety of tungstophosphates and tungstoarsenates in aqueous solution. In addition our work indicates that undoubtedly single-crystal X-ray diffraction remains the most powerful tool for the determination of novel polyoxoanion structures. It is expected that careful accumulation, interpretation, and comparison of all experimental results will be helpful in designing rational synthetic conditions for new structures. It must also be realized that polyanions containing multiple spin clusters and/or mixed-metal assemblies exhibit more complex magnetic properties than observed previously for "simpler" structures, thus opening the way for further theoretical and practical developments. Our electrochemistry studies have demonstrated that the novel compounds presented here are remarkably stable in a large pH domain compared to all other known multinickel heteropolyanions. Therefore, they constitute good candidates for electrocatalysis studies.

Acknowledgment. This work was supported by the CNRS (UMR 8000, UMR 8648, and URA 331) and the Université Paris XI. The help of Véronique Barra in running several experiments is thankfully acknowledged. U.K. thanks the International University of Bremen, Germany, for support. Figures 1−4 were generated by Diamond Version 2.1b (copyright Crystal Impact GbR).

Supporting Information Available: Three X-ray crystallographic files in CIF format and FTIR spectra of $[Ni_6As_3W_{24}O_{94}(H_2O)_2]^{17-}$, $[Ni_3Na(H_2O)_2(AsW_9O_{34})_2]^{11-}$, $[Ni_4Mn_2P_3W_{24}O_{94}(H_2O)_2]^{17-}$, $[Ni_3Na(H_2O)_2(PW_9O_{34})_2]^{11-}$, and $[A\text{-}\beta\text{-}AsW_9O_{34}]^{9-}$. This material is available free of charge via the Internet at http://pubs.acs.org.

IC0343915

(25) (a) Flanagan, J. B.; Margel, S.; Bard, A. J.; Anson, F. C. *J. Am. Chem. Soc.* **1978**, *100*, 4248. (b) Smith, T. W.; Kuder, J. E.; Wychick, D. *J. Polym. Sci*. **1976**, *14*, 2433. (c) Saji, T.; Pasch, N. F.; Webber, S. E.; Bard, A. J. *J. Phys. Chem.* **1978**, *82*, 1101.

(26) (a) Alonzo, B.; Astruc, D.; Blais, J.-C.; Nlate, S.; Rigaut, S.; Ruiz, J.; Valerio, C. *C. R. Acad. Sci., Ser. Iic: Chim.* **2001**, *4*, 173. (b) Bryce, M. R.; Devonport, W.; Goldenberg, L. M. *J. Chem. Soc., Chem. Commun*. **1998**, 945. (c) Casado, C. M.; Cuadrado, I.; Moran, B.; Alonso, B.; Garcia, B.; Gonzalès, B.; Losada, J. *Coord. Chem. Rev.* **1999**, *185*−*186*, 53.